PERGAMON

International Journal of Heat and Mass Transfer 45 (2002) 2431–2438

International Journal of HEAT and MASS TRANSFER

www.elsevier.com/locate/ijhmt

Three-dimensional convective flow adjacent to backward-facing step - effects of step height

J.H. Nie, B.F. Armaly *

Department of Mechanical and Aerospace Engineering and Engineering Mechanics, University of Missouri-Rolla, Rolla, MO 65401, USA

Received 12 September 2001; received in revised form 9 November 2001

Abstract

Three-dimensional simulations are presented for incompressible laminar forced convection flow adjacent to backward-facing step in rectangular duct and the effects of step height on the flow and heat transfer characteristics are investigated. Reynolds number, duct's width, and duct's height downstream from the step are kept constant at $Re = 343$, $W = 0.08$ m, and $H = 0.02$ m, respectively. The selection of the values for these parameters is motivated by the fact that measurements are available for this geometry and they can be used to validate the flow simulation code. Uniform and constant heat flux is specified at the stepped wall downstream from the step, while other walls are treated as adiabatic. The size of the primary recirculation region and the maximum that develops in the Nusselt number distribution increase as the step height increases. The "jet-like" flow that develops near the sidewall within the separating shear layer impinges on the stepped wall causing a minimum to develop in the reattachment length and a maximum to develop in the Nusselt number near the sidewall. The maximum Nusselt number, in the spanwise distribution, develops generally in the same region where the reattachment length is minimum. The maximum in the friction coefficient distribution on the stepped wall increases with increasing step height inside the primary recirculation flow region, but that trend is reversed downstream from reattachment. The three-dimensional behavior and sidewall effects increase with increasing step height.

1. Introduction

Flow separation and subsequent reattachment caused by sudden expansion in flow geometry, such as a backward-facing step, occurs in many engineering applications where heating or cooling is required. These applications appear in electronic cooling equipment, cooling of nuclear reactors, cooling of turbine blades, combustion chambers, environmental control systems, and many other heat transfer devices. A great deal of mixing of high and low energy fluid occurs in the separating and reattached flow regions, thus impacting significantly the heat transfer performance of these devices. Studies on separated flow have been conducted extensively during the past decade, and the backward-facing step geometry received most of the attention [1–3]. This geometry is very simple, yet the flow and the heat transfer through it contains most of the complexities that are encountered in other separating flow geometries, and for that reason it has been used in benchmark studies [4,5].

The majority of published work on separated flow deal with the two-dimensional isothermal flow, and comparatively little is published about the heat transfer for the three-dimensional flow case. Such knowledge is critical for optimizing the performance of physical heat exchanging systems because they are mostly three-dimensional and not isothermal. Iwai et al. [6] reported on the forced convection results for a duct with an aspect ratio of 16, Pepper and Carrington [7] reported results for a duct with an aspect ratio of 12, and Li and Armaly [8] reported results for a duct with an aspect ratio of 8. In addition, Iwai et al. [9] examined the effects of aspect ratio on forced convection for a fixed step height in this geometry and presented results for the Nusselt number and the shear stress. In addition, they illustrated how the

* Corresponding author. Tel.: +1-573-341-4601; fax: +1-573-341-4607.

E-mail address: armaly@umr.edu (B.F. Armaly).

0017-9310/02/$ - see front matter
PII: S0017-9310(01)00345-3

Nomenclature

AR	aspect ratio, $AR = W/s$
C_f	skin friction coefficient, $C_f = 2\tau_w/\rho u_0^2$
ER	expansion ratio, $ER = H/(H-s)$
H	Duct's height downstream from the step
h	Duct's height upstream from the step
k	thermal conductivity
L	half width of the duct
n	vector outer normal to surface
Nu	Nusselt number, $Nu = q_w s/k(T_w - T_0)$
p	pressure
Pr	Prandtl number
q_w	wall heat flux $= -k\partial T/\partial n$ at the wall
Re	Reynolds number, $Re = \rho u_0 H/\mu$
S	half height of the duct downstream from the step
s	step height
t	temperature
T_0	inlet temperature
u	velocity component in the x direction
u_0	average inlet velocity
v	velocity component in the y direction
W	width of the duct
w	velocity component in the z direction
x	streamwise coordinate axis
x_r	reattachment length
y	transverse coordinate axis
z	spanwise coordinate axis

Greek symbols

μ	dynamic viscosity
ρ	density
τ_w	wall shear stress, for three-dimensional flow $\tau_w = \sqrt{(\partial u/\partial y)^2 + (\partial w/\partial y)^2}$

"downwash" or "jet-like" flow develops through the use of streamwise velocity contours. In most of these cases the aspect ratio was too large for examining the details of the three-dimensional behavior, and the focus was on the comparison with the two-dimensional flow behavior. The effects of step height on the three-dimensional flow and heat transfer characteristics in separated flow have not been examined, and that motivated the present work.

2. Problem statement and governing equations

Three-dimensional laminar forced convection flow adjacent to a backward-facing step is simulated, and the computational domain is presented in Fig. 1. The height of the duct downstream from the step ($H = 0.02$ m) and its width ($W = 0.08$ m) were held constant throughout these simulations. By exploiting the symmetry of the flow field in the spanwise direction, the width of the computation domain was reduced to half of the actual width of the duct ($L = 0.04$ m). The length of the computational domain is 0.5 m downstream of the step and 0.02 m upstream of the step, i.e., $-2 \leqslant x/S \leqslant 50$, where S is a constant and equal to half of the duct's height downstream from the step ($S = 0.01$ m). The origin of the coordinates system is located at the bottom corner of the step where the sidewall, the backward-facing step, and the downstream wall from the step, intersect as shown in Fig. 1. Laser Doppler measurements of the flow in this geometry at $Re = 343$ and step height of 0.01 m show that the flow is laminar and steady [13], hence justifying the use of the laminar steady flow Navier–Stokes equations for this simulation.

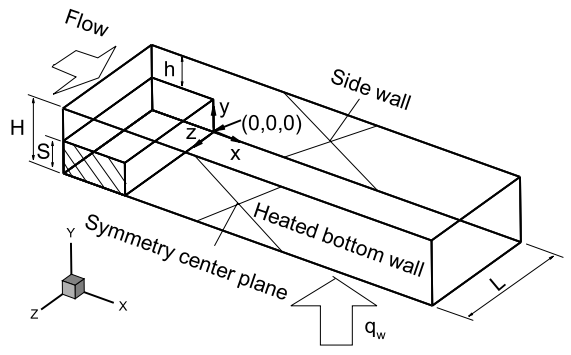

Fig. 1. Schematics of the computation domain.

The laminar steady flow three-dimensional Navier–Stokes and energy equations are solved numerically together with the continuity equation using the finite difference method.

Continuity equation

$$\frac{\partial}{\partial x}(\rho u) + \frac{\partial}{\partial y}(\rho v) + \frac{\partial}{\partial z}(\rho w) = 0. \tag{1}$$

Momentum equations:

$$\frac{\partial}{\partial x}(\rho u^2) + \frac{\partial}{\partial y}(\rho uv) + \frac{\partial}{\partial z}(\rho uw) = -\frac{\partial p}{\partial x} + \mu\left(\frac{\partial^2 u}{\partial x^2} + \frac{\partial^2 u}{\partial y^2} + \frac{\partial^2 u}{\partial z^2}\right), \tag{2}$$

$$\frac{\partial}{\partial x}(\rho uv) + \frac{\partial}{\partial y}(\rho v^2) + \frac{\partial}{\partial z}(\rho vw) = -\frac{\partial p}{\partial y} + \mu\left(\frac{\partial^2 v}{\partial x^2} + \frac{\partial^2 v}{\partial y^2} + \frac{\partial^2 v}{\partial z^2}\right), \tag{3}$$

$$\frac{\partial}{\partial x}(\rho uw)+\frac{\partial}{\partial y}(\rho vw)+\frac{\partial}{\partial z}(\rho w^2) = -\frac{\partial p}{\partial z}+\mu\left(\frac{\partial^2 w}{\partial x^2}+\frac{\partial^2 w}{\partial y^2}+\frac{\partial^2 w}{\partial z^2}\right). \quad (4)$$

Energy equation

$$\frac{\partial}{\partial x}(\rho C_p uT)+\frac{\partial}{\partial y}(\rho C_p vT)+\frac{\partial}{\partial z}(\rho C_p wT) = k\left(\frac{\partial^2 T}{\partial x^2}+\frac{\partial^2 T}{\partial y^2}+\frac{\partial^2 T}{\partial z^2}\right). \quad (5)$$

The physical properties are treated as constants and evaluated for air at the inlet temperature of $T_0 = 20$ °C (i.e., $\rho = 1.205$ kg/m^3, $C_p = 1005$ J/(kg °C), $k = 0.0259$ W/(m °C), $\mu = 1.81 \times 10^{-5}$ kg/(m s) and $Pr = 0.702$). Inlet flow upstream of the step at $x/S = -2$ is considered to be isothermal ($T_0 = 20$ °C), hydrodynamically steady and fully developed with a distribution for the streamwise velocity component (u) equal to the one described by Shah and London [10] for duct flow. The other velocity components v and w are set to be equal to zero at that inlet flow section. No slip boundary condition (zero velocities) is applied to all of the wall surfaces. Uniform and constant heat flux of $q_w = 50$ W/m^2 is specified for the stepped wall, while the other walls are treated as adiabatic surfaces. Fully developed flow and thermal conditions are imposed at the exit section of the calculation domain ($x/S = 50$) by equating the streamwise gradients of all quantities to zero at that exit flow section.

3. Numerical procedures

Staggered grid arrangement is used and the resulting finite difference equations are solved numerically by making use of a line-by-line method combined with ADI scheme [11]. SIMPLE algorithm [12] is utilized for the computation of pressure correction in the iteration procedure. Hexahedron volume elements and non-uniform grid system are employed in the simulations. The grid is highly concentrated close to the step and near the step corners, in order to insure the accuracy of the numerical simulations. Domain extension method is applied for treatment of the backward-facing step, i.e., dynamic viscosity set to a very large value for momentum equation (such as 10^{20}) and thermal conductivity set to a very small value for energy equation (such as 10^{-20}) in order to simulate the solid region during calculations. Grid independence tests were performed using several grid densities and distributions for $Re = 343$, and the primary reattachment lengths were used as the criteria. A grid of $170 \times 30 \times 30$ downstream of the step was selected for these simulations. Using a larger grid of $200 \times 50 \times 50$ downstream from the step resulted in less than 2% difference in the predicted reattachment length. At the end of each iteration, the residual sum for each of the conserved variables is computed and stored, thus recording the convergence history. The convergence criterion required that the maximum relative mass residual based on the inlet mass be smaller than 10^{-6}. All calculations were performed on a Gateway PIII 933 desktop computer with a memory of 512 Mbytes and the FORTRAN compiler is GNU 77. One iteration required approximately 14.98 s when the total number of grid points was about 1.5×10^5. The laser Doppler velocimeter (LDV) measurements by Li [13] in the simulated geometry for the case of step height of $s = 0.01$ m (expansion ratio ER = 2), and Reynolds number of $Re = 343$, were used for validating the developed computer code. Very good comparison between measured and predicted reattachment length were obtained, and that provided code validation and confidence to explore the effects of the step height on the flow and heat transfer characteristics in this geometry. The selection of this specific geometry and the flow condition ($Re = 343$) in this study was motivated by the available experimental results [13].

4. Results and discussions

Simulations are performed for different step heights ($s = 0.008$, 0.010 and 0.012 m) while holding the height of the downstream duct and the width of the duct constants. By making these changes to the step height while holding the height of the downstream duct constant at $H = 0.02$ m, resulted in the corresponding changes to the height of the upstream duct ($h = 0.012$, 0.010, and 0.008 m). This resulted in backward-facing step geometry that have expansion ratios of ER = 1.67, 2.00 and 2.50, and aspect ratios of AR = 10, 8, and 6.667, respectively. To maintain a constant Reynolds number of $Re = 343$ in the simulations while varying the step height (s), required that the average inlet velocity (u_0) and the duct's height downstream of the step (H) to be held constant. The inlet velocity profile in the upstream duct was varied, to accommodate the changes in its height, but kept as fully developed profile as proposed by Shah and London [10] while maintaining a fixed average inlet velocity ($u_0 = 0.258$ m/s) for all of the simulations' runs. Because flow measurements were available for the case of ER = 2 and $Re = 343$ [13], this Reynolds number was chosen for this study.

The negative pressure gradient that develops in the flow due to the sudden expansion at the step is responsible for developing several reverse flow regions along with swirling flow in the spanwise direction downstream from the step. The flow separates at the step and reattaches at the stepped wall forming the primary recirculation flow region. Other flow features that develop downstream from the step are shown in Fig. 2.

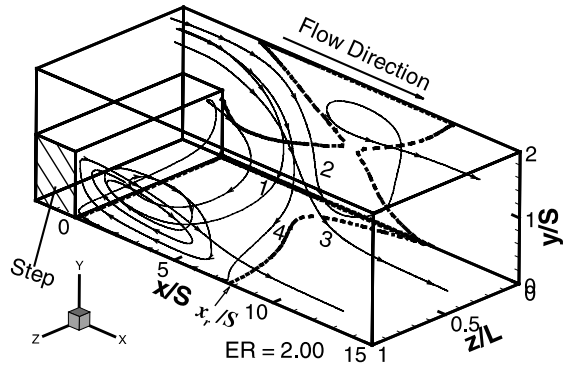

Fig. 2. Streamlines demonstrating flow features downstream from the step ($s = 0.01$ m).

This figure shows how some streamlines (flow path of particles having zero mass) that originate from the inlet section near the sidewall take different paths as they flow downstream from the step. The initial locations of the selected streamlines are listed in Table 1 and are identified by their specific number in Fig. 2.

One significant feature of the three-dimensional laminar flow adjacent to backward-facing step is the development of "jet-like" flow in the separating shear layer near the sidewall. Streamlines presented in Fig. 2 illustrate the various flow paths followed by particles that start from the locations listed in Table 1. Streamline 3 is the flow path along which a "jet-like" flow develops in the separating shear layer, impinges on the stepped wall and continues its flow downstream into the redeveloping flow region. This "jet-like" flow is responsible for the minimum and for the maximum that develop near the sidewall in the spanwise distributions of the primary reattachment length and of the Nusselt number, respectively. Streamline 2 represents flow path followed by other particles that impinge on the stepped wall, but follow a different direction than streamline 3 after impingement. These particles move toward the sidewall, after impingement on the stepped wall, while moving rapidly upward toward the top flat wall of the duct. They reverse flow direction and move upstream toward the step, and with a clockwise swirling motion move toward the center of the duct and in the downstream flow direction, thus forming a reverse and swirling flow region adjacent to the sidewall. This path is responsible for developing a maximum in the spanwise distribution of the reattachment length at the sidewall. Streamline 1 represents flow path of particles that move rapidly inside the primary recirculation flow region in a counterclockwise swirling flow that increases in size as it moves toward the center of the duct to join the flow in the downstream direction. Streamline 4 represents flow path of particles that moves rapidly across the primary recirculation flow region and directly toward the center of the duct. Close to the center of the duct, this streamline moves with the reverse flow toward the step, and then back across the duct's width toward the sidewall along the bottom corner of the step to join the counterclockwise swirling flow that exist inside the primary recirculation flow region. Major portion of the flow moves directly downstream to form the developing flow region in the duct. The results in Fig. 2 are for a step height of $s = 0.01$ m and similar results have been developed for $s = 0.008$ m and $s = 0.012$ m, but due to space limitations they are not presented here.

Table 1
Starting locations of the selected streamlines

No.	1	2	3	4
x/S	−2.00	−2.00	−2.00	−2.00
y/S	1.650	1.894	1.527	1.715
z/L	0.022	0.090	0.059	0.048

The developments of the "jet-like" flow and the reverse flow region near the sidewall, along with the effects of step height on flow characteristics, can be seen more clearly in Figs. 3 and 4. Limiting streamlines are drawn on a y-plane close to the stepped wall ($y/S = 0.01$) and on a z-plane close to the sidewall ($z/L = 0.01$) in Fig. 3. The dotted lines in these figures represent the linked points where the streamwise u-velocity component is zero on these planes. Therefore, the dotted line on the bottom y-plane ($y/S = 0.01$) is the reattachment line or the boundary of the primary recirculation flow region. The dotted lines on the z-plane close to the sidewall ($z/L = 0.01$) are the downstream and the upstream boundaries of the reverse flow region that develops adjacent to the sidewall. The "source" point that appears on the bottom y-plane in these figures is the impingement of the "jet-like" flow on the stepped wall of the duct [8]. This impingement region is the same as the region where the minimum reattachment length and the maximum Nusselt number occur on the stepped wall. The location of this jet impingement region moves further downstream of the step as the step height increases. The figures show that some streamlines flow toward and up the sidewall from the jet impingement region then reverse their directions upstream toward the step forming a reverse flow region adjacent to the sidewall. When the step is small ($s = 0.008$ m), this reverse flow region moves in a clockwise swirling flow toward the center of the duct. But, as the step height and the primary recirculation region become larger, more of the reverse flow moves back into the primary recirculation flow region following a path similar to streamline 1 that is shown in Fig. 2. The developments of a secondary recirculation flow region adjacent to the bottom corner of the step (between the primary recirculation flow region and the step) can be detected as the step height increases to a value higher than 0.008 m.

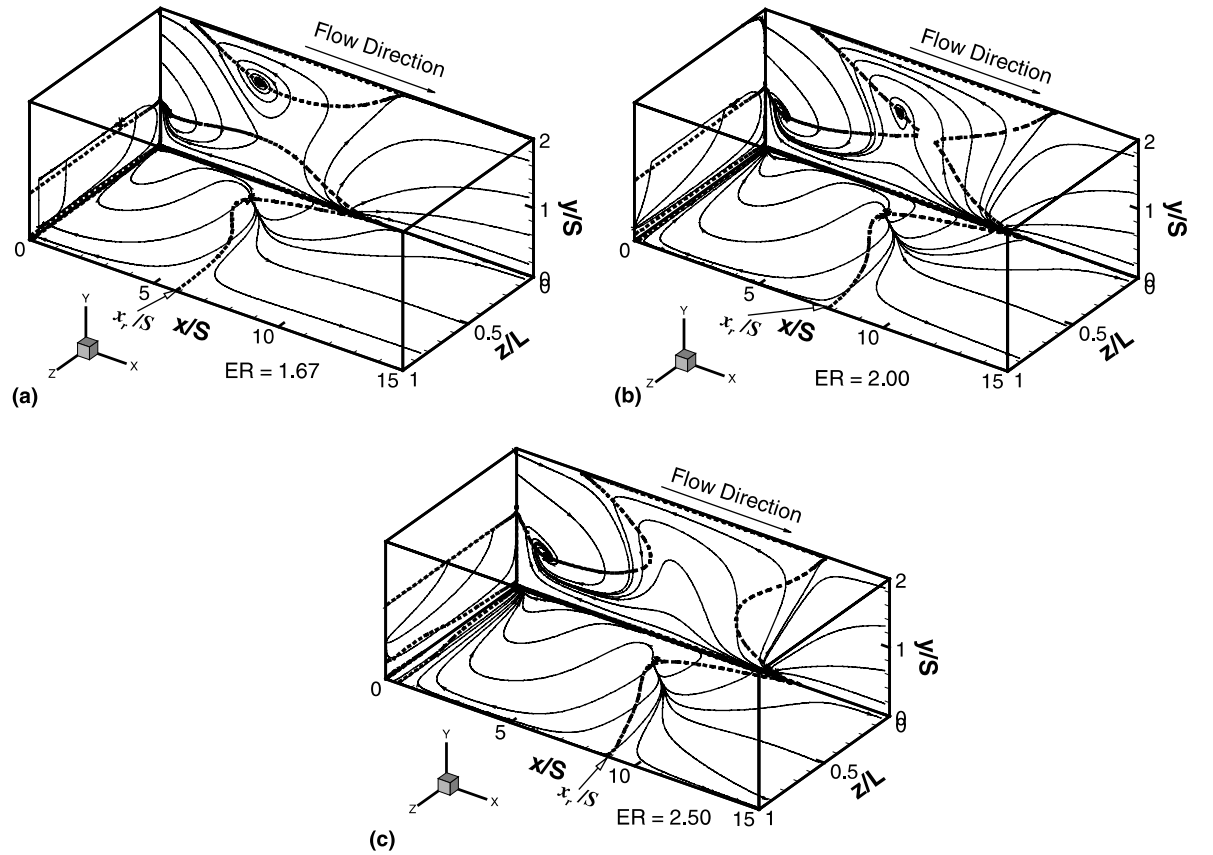

Fig. 3. Streamlines on a y-plane close to the stepped wall ($y/S = 0.01$), and on a z-plane close to the sidewall ($z/L = 0.01$): (a) $s = 0.008$ m; (b) $s = 0.01$ m; (c) $s = 0.012$ m.

Streamlines on a y-plane that is close to the upper flat wall ($y/S = 1.99$) and on a z-plane close to the sidewall ($z/L = 0.01$) are presented in Fig. 4. Interesting flow features can be seen on the y-planes of these figures. The first is an impingement region close to the sidewall. This region results from the rebound that develops when the "jet-like" flow impinges on the bottom stepped wall, causing flow to moves sharply upward toward the top flat wall as was described in Figs. 2 and 3. Reverse flow develops from that impingement region as can be seen in these figures. The impingement region on the upper flat wall moves further downstream, and the reverse flow region increases in size, in the spanwise direction as the step height increases.

The effects of step height on the primary reattachment length are presented in Fig. 5, and they show that the primary reattachment length increases with increasing step height. The locations where the "jet-like" flow impinges on the stepped wall are also shown in the figure. The minimum that occurs in the spanwise distribution of the reattachment length near the sidewall can be seen clearly in that figure and the predicted results compare very favorably with measurements for ER = 2 [13]. The maximum reattachment length occurs at the sidewall and not at the center of the duct, as one would expect. Reverse flow regions adjacent to the sidewall increase in size as the step height increases as shown in Fig. 6. The plots that are presented in this figure represent the boundaries of the reverse flow regions or lines where the streamwise velocity component is zero on a plane that is close to the sidewall ($z/L = 0.01$). The downstream boundary represents the edge where the flow reverses its direction upstream, and the upstream boundary represent the edge where the reversed flow reverses its upstream direction and starts moving in the downstream direction.

Effects of the step height on the distribution of the Nusselt number on the stepped wall are shown in Fig. 7. The dash–dotted line in these figures represents the reattachment line. As the step height increases, the maximum Nusselt number increases and its location on the stepped wall moves further downstream. The location of the maximum Nusselt number on the stepped wall is the same as the location where the "jet-like" flow impinges on the stepped wall, and where the minimum in the reattachment length develops in the spanwise direction.

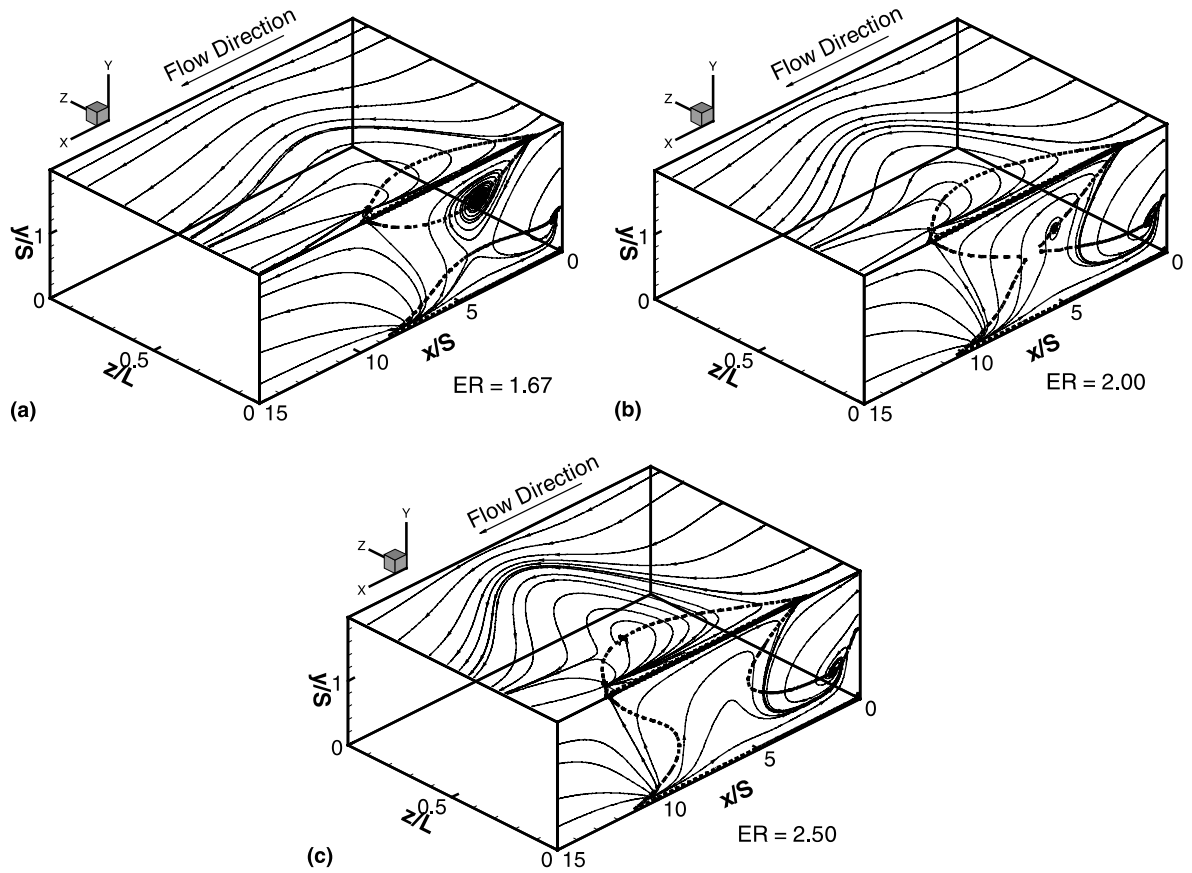

Fig. 4. Streamlines on a y-plane close to the top flat wall ($y/S = 1.99$), and on a z-plane close to the sidewall ($z/L = 0.01$): (a) $s = 0.008$ m; (b) $s = 0.01$ m; (c) $s = 0.012$ m.

The impingement of the "jet-like" flow on the stepped wall is responsible for the maximum that develops in the Nusselt number and the minimum that develops in the reattachment length. The streamwise distribution of the Nusselt number is the same as observed for two-dimensional flow with a maximum at the reattachment point and asymptotic decrease from that point to the fully developed value downstream from reattachment. An increase in the step height results in an increase in the Nusselt number. The maximum Nusselt numbers along the centerline for the three step heights and the Reynolds number considered in this study are 1.283, 1.514 and 1.822, and their positions in streamwise direction are $x/S = 6.747$, 7.612 and 8.092, respectively. The minimum value of Nusselt numbers along the centerline for

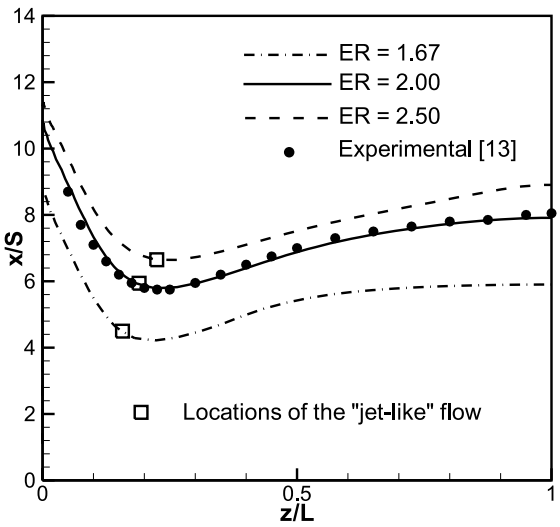

Fig. 5. Effects of step height on reattachment line.

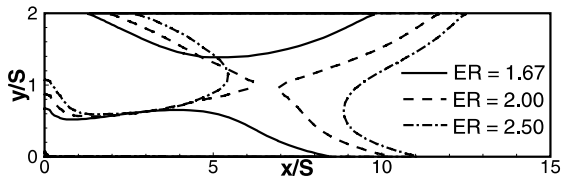

Fig. 6. Effects of step height on reverse flow region adjacent to sidewall ($z/L = 0.01$).

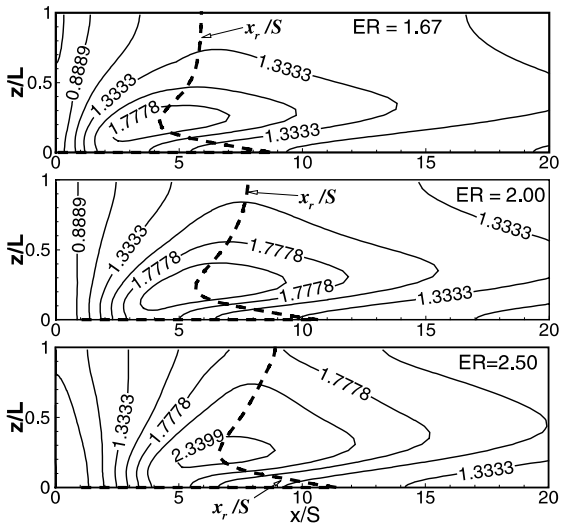

Fig. 7. Nusselt number distributions on stepped wall for $s = 0.008$, 0.01, and 0.012 m.

all three step height are located at the bottom corner of the step, i.e., intersection between the step and bottom wall. The values of the minimum Nusselt numbers for the three step heights are 0.639, 0.730 and 0.916, respectively, which are approximately half of the maximum Nusselt number for each of the cases.

The effects of the step height on the distribution of the friction coefficient on the stepped wall are presented in Fig. 8. The reattachment line is included in these figures in order to show its position relative to the minimum friction coefficient. The minimum friction coefficient lies within the same general region of the reattachment line. As step height increases, the three-dimensional feature inside the primary recirculation region becomes more pronounced. The reattachment point along the centerline of the duct is a stagnation point and the friction coefficient at that point has its minimum value of zero. The location of the minimum (zero) friction coefficient along the centerline for the three step heights are $x/S = 5.778$, 7.795 and 8.948.

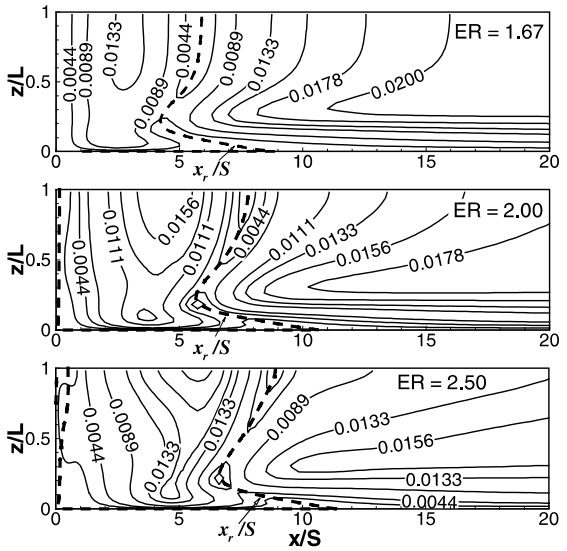

Fig. 8. Distributions of friction coefficient on stepped wall for $s = 0.008$, 0.01, and 0.012 m.

Inside the primary recirculation flow region, the maximum friction coefficient develops along the centerline of the duct and its magnitude increases as the step height increases while its position moves further downstream as the step height increases. But downstream from the reattachment line and outside the primary recirculation flow region, the friction coefficient along the centerline of the duct decreases with increasing step height. In that region the maximum friction coefficient develops close to the sidewall as can be seen in Fig. 8. For small step height, $s = 0.008$ m, the friction coefficient distribution is fairly flat in the spanwise direction inside the primary recirculation flow region, thus justifying two-dimensional approximation at the center of the duct. But as the step height increases, gradient of friction coefficient on the stepped wall inside the primary recirculation region becomes greater, both in the streamwise and spanwise directions.

5. Conclusions

Simulations of three-dimensional laminar forced convection flow adjacent to backward-facing step in a duct have been performed to study the effect of step height on the flow and heat transfer characteristics. The duct's width and height downstream from the step along with the Reynolds number were fixed at 0.08 m, 0.02 m, and 343, respectively, while the step height was varied ($s = 0.008$, 0.01, and 0.012 m). Complex three-dimensional flow develops downstream from the step with reverse and swirling flow regions adjacent to the sidewall, and a "jet-like" flow in the separating shear layer downstream from the step. The "jet-like" flow and its impingement on the stepped wall are responsible for developing a maximum in the Nusselt number and a minimum in the reattachment length. Increasing the step height increases the reattachment length, the Nusselt number, the size of the sidewall reverse flow region, and the general three-dimensional features of the flow. A secondary recirculation flow region develops adjacent to the bottom corner of the step (between the primary recirculation flow region and the step) when the step height increases. For the case of small step height ($s = 0.008$ m), the minimum Nusselt number is located near the bottom corner between the step and the

centerline of the duct. As the step height increases ($s = 0.012$ m) the minimum Nusselt number is located near the bottom corner of the step and the sidewall. Gradients in the Nusselt number inside the recirculation region increase with increasing step height. The friction coefficient increases in the streamwise direction along the centerline of the duct inside the primary recirculation flow region, but it decreases outside the recirculation region with increasing step height.

Acknowledgements

This work was supported in part by the National Science Foundation (NSF) under grants no. CTS-9906746, and CTS-9818203.

References

[1] B.F. Armaly, F. Durst, J.C.F. Pereira, B. Schonung, Experimental and theoretical investigation of backward-facing step flow, J. Fluid Mech. 127 (1983) 473–496.
[2] R.L. Simpson, Aspects of turbulent boundary-layer separation, Progress Aerosp. Sci. 32 (1996) 457–521.
[3] J.K. Eaton, J.P. Johnson, A review of research on subsonic turbulent flow reattachment, AIAA J. 19 (1981) 1093–1100.
[4] B.F. Blackwell, D.W. Pepper, Benchmark Problems for Heat Transfer Codes, ASME-HTD-222, ASME, NY, 1992.
[5] B.F. Blackwell, B.F. Armaly, Computational Aspects of Heat Transfer Benchmark Problems, ASME-HTD-258, ASME, NY, 1993.
[6] H. Iwai, K. Nakabe, K. Suzuki, Numerical simulation of buoyancy-assisting, backward-facing step flow and heat transfer in a rectangular duct, Heat Transfer – Asian Res. 28 (1999) 58–76.
[7] D.W. Pepper, D.B. Carrington, Convective heat transfer over a 3-D backward facing step, in: G. de Vahl Davis, E. Leonardi (Eds.), Proceedings of the ICHMT International Symposium on Advances in Computational Heat Transfer, 1997, pp. 273–281.
[8] A. Li, B.F. Armaly, Convection adjacent to a 3-D backward-facing step, in: Proceedings of the ASME/AIChE National Heat Transfer Conference, NHTC 2000-12301, 2000.
[9] H. Iwai, K. Nakabe, K. Suzuki, Flow and heat transfer characteristics of backward-facing step laminar flow in a rectangular duct, Int. J. Heat Mass Transfer 43 (2000) 457–471.
[10] R.K. Shah, A.L. London, Laminar Forced Convection in Ducts, Academic Press, New York, 1978.
[11] S.V. Patankar, Numerical Heat Transfer and Fluid Flow, Hemisphere, New York, 1980.
[12] S.V. Patankar, D.B. Spalding, A calculation procedure for heat, mass and momentum transfer in three-dimensional parabolic flows, Int. J. Heat Mass Transfer 15 (10) (1972) 1787–1806.
[13] A. Li, Experimental and numerical study of three-dimensional laminar separated flow adjacent to backward-facing step, Ph.D. thesis, University of Missouri, Rolla, MO, 2001.